**Article:**

Cascant, Mari Merce, Rubio, Sonia, Gallello, Gianni et al. (3 more authors) (2017) Burned bones forensic investigations employing near infrared spectroscopy. Vibrational Spectroscopy. pp. 21-30. ISSN 0924-2031

https://doi.org/10.1016/j.vibspec.2017.02.005

# BURNED BONES FORENSIC INVESTIGATIONS EMPLOYING NEAR INFRARED SPECTROSCOPY

Mari Merce Cascant[1], Sonia Rubio[1], Gianni Gallello[1,2]*, Agustín Pastor[1], Salvador Garrigues[1] and Miguel de la Guardia[1].
[1]Department of Analytical Chemistry, University of Valencia,
50 Dr. Moliner Street, research building
46100 Burjassot, Valencia, Spain.
[2] Department of Archaeology, University of York,
King's Manor, York YO1 7EP, UK.
* Corresponding author

***Corresponding author: Gianni Gallello**
**Tel.+34697636957**
**Fax+34 96 3544838**
**Email: gianni.gallello@uv.es**

## Abstract

The use of near infrared (NIR) spectroscopy was evaluated, by using chemometric tools, for the study of the environmental impact on burned bones. Spectra of internal and external parts of burned bones, together with sediment samples, were treated by Principal Component Analysis and cluster classification as exploratory techniques to select burned bone samples, less affected by environmental processes, to properly carry out forensic studies. Partial Least Square Discriminant Analysis was used to build a model to classify bone samples based on their burning conditions, providing an efficient and accurate method to discern calcined and carbonized bone. Additionally, Partial Least Square regression models were built to predict calcium, magnesium and strontium concentration of bone samples from their NIR spectra, being obtained an accurate root mean square error of prediction of 5.2% for calcium. Furthermore a screen methodology, for magnesium and strontium prediction, with a RPD of 0.24 and 1.08 respectively, was developed.

**Keywords:** Burned bones, FT-NIR, chemical elements, statistics.

## 1. Introduction

The analysis of burned human remains is of great interest among forensics and anthropologists due to the problems associated to their recovery, identification and classification [1]. Burned bone samples provide knowledge of changes in bone in order to use this information for anthropological and forensic studies [2]. Consequently, during the last decades, the number of published papers on burned bone analysis has increased [3-5].

Burned bones could be classified as carbonized and calcined depending on the thermal exposure, exhibiting a black appearance (carbonized) due to skeletal material and soft tissue or a white appearance (calcined). Burned bones are incinerated when the thermal alteration is so prolonged and intense that all the organic materials and moisture were lost [6, 7]. Estimation of the maximum exposure temperature is a crucial factor for the correct interpretation of burned bones, being the change of colour an employed method as temperature range indicator [6, 8]. Colour has been described qualitatively by visual comparison with standard charts, such as the Munsell Soil Color Charts [9]. However different perceptions or changes in lighting conditions can significantly modify the results [6]. Another method used to colour determination was suggested by Devlin et al. [10] using CIE L*a*b* (CIELAB) uniform colour space for the recording of bone surface colour data. However, mistakes on the methodologies employed for burned bone classification and analysis have recently been stressed. Some authors indicate that colour of bone fragments is a combination of temperature, duration of elevated temperature treatments, oxygen presence during combustion and context of incineration. All those factors should be considered [11, 12]. Nicholson [13] found the colour changes greatly varied between bones, attributing these observations to different organic content and bone chemistry. Symes et al. [14] indicate that different colour alterations can be found within a single skeleton and even on a single bone, especially in cases of burning of fleshed remains. Also, other aspects, as external and diagenetic factors, could modify the bone colour producing similar changes than those caused by high temperatures [15-17]. Overall, study of burned remains is a difficult interpretative challenge for forensics and anthropologist due to different factors and aspects to be considered.

As the temperature increases, the hydroxyapatite present in bones has an increased crystallinity and forms stable and large crystals [18], starting the most important transformation at $600^{o}$ C [11]. Lanting et al. [19] perceived the potential of calcined bones for radiocarbon dating, indicating that all previous attempts to date burned bones failed because they were treated as carbonized bones. Exchange processes of bicarbonate ions dissolved in soil waters produce a bio-apatite contamination which results in too young $^{14}$C dates, not occurring that on calcined bones [20]. During the last decade an increment of calcined bones radiocarbon dating studies has been produced [21-24].

Several studies were carried out to understand the bone mineral elements behaviour under thermal conditions and the influence of post-depositional processes in skeletal remains [25-28]. Some works have shown that post-mortem processes equally affect cremated and non-cremated ancient bones [27, 28]. Elemental composition studies made on incinerated bones were carried out by Grupe et al. [25], concluding that paleodietary reconstruction is limited due to volatilization and crystal modifications caused by high temperatures. However, for Sr/Ca, a ratio which is the most used method for palaeodietary reconstruction, it is possible to use regression analysis.

Indeed, the presence of hydroxyl groups in bone apatite continues to be a topic of controversy. Some studies believe that a number of hydroxyl groups are present in archaeological bones [29, 30] while others argue that bone apatite does not contain detectable concentrations of hydroxyl groups [31, 32]. Hydroxylation of bone apatite is attributed to the presence of $CO_3^{2-}$, according to two substitution mechanisms in the $OH^-$ site, through the so called “A-type” substitution, or in the $PO_4^-$ site, based on “B-type” substitution[31]. Other exchanges, such as fluoride ($F^-$) substitution for hydroxide ($OH^-$), and strontium ($Sr^{2+}$) and other trace cations ($Zn^{2+}$, $Pb^{2+}$) substitution for calcium ($Ca^{2+}$), are also produced [33].

Additional studies are needed to get deep information on the mineral composition of remains, crystallinity of samples and the influence of soil component exchanges. Infrared spectroscopy (IR) has been used to assay the modifications of bone apatite during calcinations, mostly on experimentally heated bone [34-36]. However, the relative impacts of temperature and exposure time remain unclear and IR could be also useful to evaluate the presence of major mineral elements in bone remains.

The aim of the present study has been to select the most suitable samples to carry out forensic studies and, to do it, the evaluation of near infrared spectroscopy has been employed being used chemometric tools as Principal Component Analysis (PCA), Cluster Analysis (CA) and Partial Least Squares-Discriminant Analysis (PLS-DA). Carbonized bones are more prone than calcined ones to degradation by exchange processes with soil, for that a classification of bones allows ensuring analysis results. Internal part, external part of burned bones and sediment samples were analysed for a better understanding of post-mortem bone modification processes. Furthermore, it has been evaluated the simultaneous determination of calcium, magnesium and strontium in burned bones by PLS-NIR in order to provide environmentally friendly screening tools to evaluate the presence of mineral elements in bones.

## 2. Material and methods

### 2.1. Samples

Thirty-eight burned bone samples, from Corral de Saus Necropolis were studied [28]. This site was dated between the III and II centuries B.C., a period in which cremations were placed in urns where each one contained the remains of a single individual. Bones were divided into “carbonized”, bones fired in reducing atmosphere, “calcined”, those fired in oxidizing atmosphere and “unknown”, for bones of unidentified burning conditions.

Additionally, unburned animal bones and sediments were obtained from the inside of urns, mixed with ashes, carbons and human bones. To carry out the study fifteen internal part of bones (seven carbonized and eight calcined), seven external part of bones (being obtained from the first 2 mm of bone directly in contact with the sediments), seven unknown bones, four unburned animal bones and six sediment samples were used. Additionally, 31 unknown samples from Las Peñas Necropolis [37] were analysed and the certified material Bone ash NIST 1400 and soil GBW07408 were used for evaluating the analytical method.

### 2.2. Apparatus and methods

A Fourier transform near infrared (FT-NIR) spectrometer, model Multipurpose Analyzer (MPA) from Bruker (Bremen, Germany) equipped with an integrating sphere, was employed for diffuse reflectance near infrared spectra acquisition. For instrumental and measurement control of the spectrometer, as well as for data acquisition, Opus 6.5 software from Bruker was used.

Optima 5300 DV Inductively Coupled Plasma Optical Emission Spectrometry (ICP-OES) Perkin Elmer (Norwalk, CT, USA) equipped with an autosampler AS 93-plus and a cross flow nebuliser was used to obtain reference values on the mineral composition of samples. Samples were previously calcined in a muffle furnace Biometa Lenton ECF 12145A (Lanera, España) and digested with acids using a heating plate Ika C-Mag HS7 (Staufen, Germany).

### 2.3. Reference method

Samples were analysed after acid digestion using ICP-OES. The digestion method consisted of the addition of 1.5 ml HCl and 1.5 ml $HNO_3$ to 0.5g of sample in glass tubes, for both, bones and soil. Digestion of samples was carried out in a water bath at 100$^{o}$ C for 40 min. The digested solutions were quantitatively transferred to plastic tubes and diluted to a final volume of 15 ml with distilled water. Concentration ranges of the dilutions from the digested solution were adapted to the sensitivity of the ICP-OES measurements for each element. From a multi-elemental stock solution containing Ca, Mg and Sr of 100 μg $ml^{-1}$ calibration standards were prepared by the appropriate dilution, also adding $HNO_3$ and HCl at the same level of samples. Standards were obtained from Sharlab S.L. (Barcelona, Spain). Reference materials bone ash NIST 1400 and soil NIM GBW07408 were used to evaluate the accuracy of the analytical method. Re was used as internal standard in ICP-OES [28]. Mineral content of samples, determined by reference method, were between the range of 250 and 461 mg $g^{-1}$ for calcium, 790 and 34257 μg $g^{-1}$ for magnesium and, 161 and 1068 μg $g^{-1}$ for strontium.

### 2.4. NIR procedure

NIR spectra were directly obtained by diffuse reflectance in Kubelka–Munk units from pulverized samples placed inside glass vials of 11 mm internal diameter and 25 mm height. Sample spectra were obtained from 14000 to 4000 $cm^{-1}$ by averaging 50 scans per spectrum using a nominal resolution of 4 $cm^{-1}$, as instrumental conditions. The background spectrum was acquired from the integrating sphere under the same instrumental conditions than those employed for sample measurements. Three measurements of each sample were obtained by rotating the sample vial position between replicates in order to ensure a better reliability. The means of the triplicate spectra of each sample were employed for chemometric treatment.

### 2.5. NIR Quality Control (QC)

Bone samples were measured in triplicate. Certified reference material Bone ash NIST 1400 was measured under the same conditions than samples in three different times during each measurement session during 18 days: at the beginning of the session, in the middle and at the end of measurements. In order to evaluate the proposed method, inter-day precision and accuracy of measurements obtained for Bone ash NIST 1400 were used. Precision was expressed as the coefficient of variation of the results obtained during 18 different days and accuracy was expressed as the bias between the predicted and the certified value divided by the certified value, expressed as percentage.

### 2.6. Chemometric data treatment

Data treatment was done with Matlab 8.3.0.532 (R2014a) from Mathworks (Natick, MA, USA) using PLS Toolbox 7.5.2 from Eigenvector Research Inc. (Wenatchee, WA, USA) for Principal Component Analysis (PCA), cluster classification, Partial Least Square Discriminant Analysis (PLS-DA) and Partial Least Squares (PLS) regression in order to do a correct identification of samples and for the quantitative prediction of Ca, Mg and Sr concentrations in bones from sample NIR spectra.

PCA allows a reduction of variables and provides projection of data in a new space related to the minimum of independent variables suitable to explain an appropriate amount of data variance, so that, enhancing and easing data exploration and interpretation [38].

Cluster Analysis differs from PCA in its capability to detect similarities between samples and to define groups of samples from their spectra. Similarities among samples are estimated by means of distances: similar samples are characterized by small distances and the opposite for dissimilar ones. The dendrograms obtained encode the cluster structure of data and the partition of samples is obtained by cutting the dendrogram at the desired level of similarity [38].

PLS-DA is a linear classification method that combines the properties of partial least squares regression with the discrimination power of a classification technique [39]. The main goal of PLS-DA is to build a calibration model suitable to be applied in future classifications. A series of parameters can be used to evaluate the performance of classification models as true positive (TP) and true negative (TN), false positive (FP) and false negative (FN) classification results, sensitivity, specificity, accuracy, efficiency, and

Matthews correlation coefficient (MCC). The TP rate is the probability that a positive sample can be classified as positive, TN involves that a negative sample can be classified as negative. A similar criterion is employed to determine FN and FP rates. Sensitivity is the ability of the model to correctly classify authentic samples inside their group using the TP and FN rate. Specificity is the capacity of the model to correctly identify samples relative to the values of TN and FP. The accuracy is the rate of correct classification, independently of the class of sample. The efficiency and MCC summarize the model performance. The efficiency was determined as the arithmetic average of the values of sensitivity and specificity, where a value of 1 corresponds to an efficiency of 100%. MCC gives a value between -1 and +1, where a value of +1 represents perfect classification, 0 an erroneous classification and -1 an inverse classification [40, 41].

PLS regression was applied to NIR data in order to develop prediction models for calcium, magnesium and strontium content in bone samples. Different spectra pre-processing, including multiplicative scatter correction (MSC), standard normal variation (SNV), a Savitzky-Golay first (FD) and second derivative (SD), and mean center (MC), were tested to treat raw data prior to the PLS regression using different spectral regions. The performance of PLS-NIR models was evaluated according to the root mean square error of cross validation and prediction (RMSECV and RMSEP), the correlation coefficient of prediction ($R^2$pred), relative root mean square error of prediction (RRMSEP) and residual predictive deviation (RPD), calculated as the ratio between standard deviation (SD) of the prediction set and the RMSEP values [42].

## 3. Results and discussion

### 3.1. NIR spectra

Figure 1 shows the NIR spectra of: a) calcined bone, b) carbonized bone, c) superficial part of bone, d) animal bone and, e) sediment samples, in the region between 9000-4000 $cm^{-1}$ without any data pretreatment. The spectra region between 5500 and 8000 $cm^{-1}$ corresponds to the first fundamental overtone of the mid-infrared OH stretching vibration, the region between 4000 and 5500 cm$^{-1}$ is ascribed to the water OH overtones and carbonate combination bands, and the region between 8000 and 12000 cm$^{-1}$ is related to the second fundamental overtone of the OH stretching vibrations and also includes electronic bands resulting from the presence of transition metal ions in the structure [43]. Position and assignment of the different bands is given in Table 1 [44-47]. Main differences found between burned bones as a function of their treatment are based on the band located at 6977 cm$^{-1}$, assigned to the first overtone of the stretching vibrations of OH group in hydroxyapatite. This band is higher in calcined bones than in carbonized ones. Additionally, the band at 5275 cm$^{-1}$ is related to apatite, present in carbonized bones and not in calcined ones. These two differences can indicate the substitution of $CO_3^{2-}$ in the $OH^-$ site through A-type substitution due to the loss of hydroxylation degree during the carbonization process, being these bones less resistant to diagenetic alteration than calcined ones.

## 3.2. Exploratory analysis:

### 3.2.1. Principal component analysis (PCA)

PCA is nowadays the most common chemometric strategy for unsupervised exploratory data analysis. Scores plot often gives a good view of how the trends from different components relate to each other. Figure 2 shows the scores plot for first and second principal components obtained from PCA treatment of NIR spectra of samples from Corral de Saus and Las Peñas Necropolis. After FD and MC pre-treatment and, selecting the region from 9000 to 4000 cm$^{-1}$, the two first principal components represent 72.61 % of the explained variance, being 41.39 % and 31.22 % explained by PC1 and PC2, respectively. It can be appreciated that NIR spectra of sediment samples are clearly different from those of internal part of bone samples in the direction of PC1 and that, a few spectra of external part of bone samples are located near of sediment and others near of the internal part of bones. As It has been already evidenced [28] this indicates that external part of bones had undergone stronger changes than internal ones due to digenetic factors. Also, in the direction of PC2 it can be seen that calcined bone sample spectra from Corral de Saus are located down, and carbonized bone spectra are placed up. Additionally, Las Peñas bone spectra are located close to these of internal part of bones from Corral samples It indicates similarities between these two groups. The same can be observed for SRM Bone ash NIST 1400 spectrum. Figure 3 shows loading plots in order to understand the distribution of samples in PCA, indicating that responsible wavenumbers are ones around 7000 $cm^{-1}$ and between 5500 and 4000 $cm^{-1}$. Consequently, it can be seen that PCA analysis using NIR offers a fast and green tool to identify changes in bones caused by environmental factors.

### 3.2.2. Hierarchical cluster analysis (HCA)

Hierarchical cluster analysis (HCA) involves a measurement of the similarity between objects to be clustered, and thus samples with the maximum similarities in their NIR spectra were clustered together preferentially. Figure 4a shows the dendrogram obtained from samples of Corral de Saus after FD and MC pre-treatment of NIR spectra and selecting the region from 9000 to 4000 $cm^{-1}$, using the average-paired as a distance measure. It can be seen that for a minimum cut off value of 0.016, all samples were classified into two main groups, which correspond to samples with common characteristics, like sediment and bones. The first group incorporates all sediments. However, it also included 5 samples of external part of bones, probably because these samples were altered by environmental factors. The second group is based on internal part of bone spectra, where it can be seen animal ones together with carbonized and calcined bones with also unknown samples and 2 external parts of bones. Additionally, it can be appreciated general trends in the behaviour of samples. For a cut-off value of 0.012 samples were classified as sediments, animal bones and internal part of bones. For a cut-off value of 0.0075, samples were classified as calcined and carbonized bones. From the aforementioned facts it can be concluded that samples similar to sediments, as external part of bones, are included in this group, and samples different to the soil, as calcined bones, are placed in the opposite part of the dendrogram obtained from NIR spectra. So that, HCA indicates that calcined bones presents fewer structural changes than carbonized and external part of bones.

Furthermore, Figure 4b shows a dendrogram established from spectra of internal part of bone samples that was build using a K-means nearest group as distance measure. Here, it can be appreciated that for a minimum cut off value of $8 \cdot 10^{-3}$, samples were classified into two main groups corresponding to calcined and carbonized bones, respectively.

### 3.3. Partial least squares for discriminant analysis (PLS-DA)

The main goal of PLS-DA is to build a calibration model that could be applied in future classifications. Burned bone class assignments are not always possible by looking at the remains colour. PLS-DA can be applied to classify bone samples depending from their burning conditions. A Calibration set was built using NIR spectra of internal bones of Corral de Saus assigned to the classes “calcined” and “carbonized”. Leave-one-out cross-validation method was used in the training set to select the number of latent variable in the PLS-DA. Figure 5 illustrates the classification for PLS-DA, after FD and MC pre-treatment and selecting the region from 9000 to 4000 $cm^{-1}$. It can be seen a good class separation between calcined and carbonized bones, obtained using one latent variable which explains 70.83 % of the total variance of the X data block and 83.56 % of the Y data block. Sensitivity and specificity results for classification using PLS-DA were 100 % for both, calibration and cross validation sets, obtaining satisfactory results in the classification of samples into true positive and negative classes. It indicates excellent separation of the classes. The efficiency and accuracy were 100 % and the MCC had a value of 1. Additionally, PLS-DA model was validated employing permutation testing using 30 iterations and one latent variable. p-values of 0.010 and 0.008 were obtained for self-prediction and cross-validation, respectively, by employing, a randomization t-test for evaluating residuals, thus confirming the significance of the original PLS-DA model at a 95 % confidence level.

The aforementioned model was applied to evaluate the NIR spectra of bone samples of unknown burning conditions derived from Corral de Saus and Las Peñas Necropolis, together with unburned animal bone samples. As it can be appreciated from Figure 5, all animal bone samples were similar to carbonized bones, whereas some of the unknown bones were assigned to the class of calcined bones and others to the class of carbonized bones.

Therefore, it can be concluded that PLS-DA allows a screening classification to assign bone class as calcined or carbonized, avoiding the confusing visual interpretation. So that, as the calcined bones are more resistant to diagenetic alteration due to their high cristallinity, PLS-DA permits to do an adequate selection of bones in order to ensure forensic studies that could comprise biological or radiocarbon dating investigations, additionally than studies based on the mineral composition of human remains concerning cultural aspects as diets or life habits.

### 3.4. Prediction of major elements by Partial Least Squares (PLS) regression model

PLS regression models were built to predict the presence of major elements in bone samples from their NIR spectra. A total of 38 samples of Corral de Saus Necropolis were used as calibration set. To confirm the suitability of the chosen preprocessing strategy for model building, 31 samples of Las Peñas Necropolis were employed as external validation set. Table 2 shows the descriptive statistics mean, standard deviation (SD) and range of concentration for the determination of Ca, Mg and Sr in samples included in the calibration and validation sets. Additionally, a sample of Bone ash NIST 1400 was used as standard reference material for evaluating accuracy of the analytical procedure.

Different spectral regions and pre-processing strategies were applied to build the best models to evaluate Ca, Mg and Sr concentration in burned bones. For all elements determination, regions selected were those between 9000 and 4000 cm$^{-1}$. In all cases, FD was calculated with a window of 15 points and second order polynomial, together with

MC treatment, were adopted as signal pre-processing. Models with 3, 8 and 3 latent variables (LVs) were selected for calcium, magnesium and strontium, respectively and these LVs achieved an explained variance of 72.62 %, 95.9 % and 87.61 % for X variables and 72.77 %, 99.61 % and 80.90 % for Y variables, respectively. Outliers can be identified by Q residual versus the Hotelling T2 values, being removed 3 samples prior to build calibration models of Ca and Sr and 2 samples, in the case of Mg. Moreover 2 samples were removed for validation set of Sr. Figure 6 shows the correlation among the predicted and reference values for the concentrations of Ca, Mg and Sr for the calibration and validation sets, with good coefficients of determination of calibration ($R^2$cal), cross validation ($R^2$CV) and prediction ($R^2$pred). Acceptable RRMSEP values were obtained for calcium with 5 % mean values. However, average relative prediction, for Mg and Sr, provided high values of RRMSEP, with RPD values of 0.86, 0.24 and 1.08, respectively for the three elements under study. The most important calibration and validation parameters of the developed PLS-NIR models are summarized in Table 3.

### 3.5. NIR Quality Assurance and Quality Control (QA/QC)

Inter-day precision and accuracy of PLS regression models to predict Ca, Mg and Sr were evaluated from the analysis of archeological samples and a reference one. CV varies from 0.2 % till 1.8 % for Ca and Sr, being data found for Mg between 4.7 % and 13.8 %. On the other hand the bias obtained for the reference material was lower than 10 % in the case of Ca and Sr determination being obtained a range of relative errors between -4.3 % and -2.3 % for Ca and from 6.9 % till 9.9 % for Sr. In the case of Mg the accuracy relative errors varied from -26.5 % till -8.4 %. Moreover, PCA could evaluated the precision of the method by visualization of data projection due to the fact that replicates were placed all together and near of calcined bones.

### 3.6. Evaluation of methods

The developed NIR methodology allowed us to identify the best preserved samples and to predict Ca, Mg and Sr in burned bones. However it is necessary to evaluate advantages and drawbacks of the proposed methodology versus the reference one and in fact it can be concluded that NIR spectroscopy methodology is faster than ICP-OES for sample preparation and measurement and to obtain results. However, the lack of NIR sensitivity is the main limitation of the method, being only the major components of bones as Ca, Mg and Sr able to be determined and not the trace ones.

Moreover, evaluation of the proposed NIR procedure and the ICP-OES reference methodology was made by comparing them according by the so called Green Certificate. The greenness of the analytical methodologies were evaluated by using the eco-scale proposed by Van Aken et al. [48], developed by Galuszka et al. [49] and modified by Armenta et al. [50] to establish the Green Certificate. It includes a new criterion to quantify the penalty point values and associate the eco-scale value to a category class from A to G. Figure 7 shows the results of the green evaluation of FT-NIR and ICP-OES. One penalty point was assigned to FT-NIR due to the consume of energy by the mineralization of samples in muffle furnace. The NIR procedure has a category class A on the Green Certificate with a mark of 99. For ICP-OES, the final mark was of 86.5 due to 2 penalty points assigned for the use of $HNO_3$ and HCl in the sample treatment, the use of standard solutions and argon for plasma generation; 3 penalty points due to the consume of energy by the muffle furnace and ICP-OES and 8.5 penalty points due to the wastes. So, ICP-OES can be considered as a B class in Green Certificate ranking.

### 3.7. Forensic applications

Forensic anthropologists correlate the maximum exposure temperature of bones remains with colour changes to obtain a correct interpretation of burned bones. This estimated temperature could be a difficult task being a subjective and confusing method due to different factors that should be considered such are; time, temperature, oxygen availability and external and diagenetic factors. PLS-DA by using NIR spectra permits an accurate burned bone classification avoiding the confusing colour interpretation.

Calcined bones are more resistant to environmental alterations than carbonized ones being thus calcined bones more adequate for investigation studies about radiocarbon dating and diet reconstruction by using Sr/Ca ratio. PCA analysis using NIR offers a fast and green tool to identify changes in bones caused by environmental factors. Therefore, an appropriate selection of samples could avoid interpretative errors related to the structure and chemical composition of bones that could be post-mortem modified by diagenetic factors.

On the other hand, the use of PLS-NIR as a screening methodology for Ca, Mg and Sr estimation offer an additional value to the use of NIR spectra in bone remains studies.

## 4. Conclusions

Interesting results were obtained using PCA, HCA and PLS-DA to classify burned bones. PCA, using two principal components, was able to discriminate bone remains affected by post depositional diagenetic processes to those relatively free due to their lack of exchanges with the soil components. HCA permitted to clearly separate calcined and carbonized bones and could be useful to roughly understand the thermal treatment of unknown remains. PLS-DA multivariate provided an accurate tool to discriminate between calcined and carbonized and to classify accurately unknown burned bones.

From a prior study concerning buried bones from two late roman necropolises [51] the use of NIR spectroscopy combined with chemometrics provides a rapid and cost efficient method to screen the concentration of calcium, magnesium and strontium also in burned bones aiming to understand post-mortem changes by environmental degradation.

In short, it can be concluded that the proposed methodologies, based on the use of NIR spectroscopy combined with chemometric tools provide fast and green approaches to select the most suitable samples for forensic studies and evaluation of major mineral elements in bone remains. It is very important due to the fact that carbonized bones are more prone than calcined ones to post-depositional processes and those can produce mistakes during data interpretations. Additionally, PLS regression models built from NIR spectra provided a screening tool to predict Ca, Mg and Sr in burned bones.

## Acknowledgements

Authors acknowledge the financial support of Generalitat Valenciana (Project **PROMETEO II/2014/077**) and **Ministerio de Economia y Competitividad-Feder** (Projects **CTQ 2014-52841-P**). M.C acknowledges the FPI grant (**BES-2012-055404**) provided by the **Ministerio de Economia y Competividad** of the Spanish government.

The authors would like to thanks all the students of Chemistry and Archaeology which have contributed to the realization of this study.

## References

[1] S. A. Symes, D.C. Dirkmaat, S.Ousley, E. Chapman M.S, and Luis Cabo M.S, The Analysis of Burned Human Remains, San Diego, US Department of Justice, 2012.

[2] T.J.U. Thompson, Heat-induced Dimensional Changes in Bone and their Consequences for Forensic Anthropology, J Forensic Sci, 50(2005) 1008–15.

[3] D. Gonçalves, T.J.U. Thompson, and E. Cunha, Implications of heat-induced changes in bone on the interpretation of funerary behaviour and practice, J. Archaeol. Sci., 38(2011) 1308–1313.

[4] T.J.U. Thompson, Recent advances in the study of burned bone and their implications for forensic anthropology, Forensic Sci. Int., 146(2004) Supplement, S203–S205

[5] D.H. Ubelaker, The forensic evaluation of burned skeletal remains: A synthesis, Forensic Sci. Int.,183(2009) 1–5.

[6] S.T.D. Ellingham, T. J. U. Thompson, M. Islam, and G. Taylor, Estimating temperature exposure of burnt bone — A methodological review, Sci. Justice, 55(2015) 181–188.

[7] S. A. Symes, C. W. Rainwater, E. N. Chapman, D. R. GIipson, and A. L. Piper, Chapter 2. Patterned thermal destruction of human remains in a forensic setting, in The Analysis of Burned Human Remains, San Diego: Academic Press, 2008.

[8] P. Shipman, G. Foster, and M. Schoeninger, Burnt bones and teeth: an experimental study of color, morphology, crystal structure and shrinkage, J. Archaeol. Sci., 11(1984) 307–325.

[9] M. Color, Munsell Soil Color Charts. New Windsor, N.Y, Macbeth Division of Kollmorgan Instruments Corp, NY, 1994.

[10] J. B. Devlin and N. P. Herrmann, Chapter 6. Bone color as an interpretive tool of the depositional history of archaeological cremains, in *The Analysis of Burned Human Remains*, San Diego: Academic Press, 2008.

[11] R. F. Castillo, D. H. Ubelaker, J. A. L. Acosta, and G. A. C. de la Fuente, Effects of temperature on bone tissue. Histological study of the changes in the bone matrix, Forensic Sci. Int., 226(2013) 33–37.

[12] P.L. Walker, K.P. Miller, Time, temperature, and oxygen availability: an experimental study of the effects of environmental conditions on the color and organic content of cremated bone, Am. J. Phys. Anthropol. Suppl. 40 (2005) 216–217.

[13] R. A. Nicholson, A Morphological Investigation of Burnt Animal Bone and an Evaluation of its Utility in Archaeology, J. Archaeol. Sci., 20(1993) 411–428.

[14] S.A. Symes, C.W. Rainwater, E.N. Chapman, D.R. Gipson, A.L. Piper, Patterned thermal destruction of human remains in a forensic setting, in: C.W. Schmidt, S.A. Symes (Eds.), The Analysis of Burned Human Remains, Academic Press, London, 2008, 15–54.

[15] J.B. Devlin, N.P. Herrmann, Bone color as an interpretive tool of the depositional history of archaeological cremains, in: C.W. Schmidt, S.A. Symes (Eds.), The Analysis of Burned Human Remains, Academic Press, London, 2008 , 109–128.

[16] R. Shahack-Gross, O. Bar-Yosef, S. Weiner, Black-coloured bones in Hayonim Cave, Israel: differentiating between burning and oxide staining J. Archaeol. Sci., 24(1997), 439–446.

[17] C.K. Brain, A. Sillen Evidence from the Swartkrans cave for the earliest use of fire Nature, 336 (1988), 464–466.

[18] K. A. Gross and C. C. Berndt, Biomedical Application of Apatites, Rev. Mineral. Geochem., 48(2002) 631–672.

[19] Lanting, J.N., Aerts-Bijma, A.T., van der Plicht, J., Dating cremated bone, Radiocarbon 43(2001) 249–254.

[20] T. A. Surovell, Radiocarbon dating of bone apatite by step heating, Geoarchaeology, 15(2000) 591–608.

[21] G. Quarta, L. Calcagnile, M. D'Elia, L. Maruccio, V. Gaballo, and A. Caramia, A combined PIXE–PIGE approach for the assessment of the diagenetic state of cremated bones submitted to AMS radiocarbon dating, Nucl. Instrum. Methods Phys. Res. Sect. B Beam Interact. Mater. At., 294(2013) 221–225.

[22] A. Zazzo and J.-F. Saliège, Radiocarbon dating of biological apatites: A review, Palaeogeogr. Palaeoclimatol. Palaeoecol., 310(2011) 52–61.

[23] J. Olsen, K. M. Hornstrup, J. Heinemeier, P. Bennike, and H. Thrane, Chronology of the Danish Bronze Age Based on 14C Dating of Cremated Bone Remains, Radiocarbon, 53(2011) 261–275.

[24] J. Olsen, J. Heinemeier, P. Bennike, C. Krause, K. Margrethe Hornstrup, and H. Thrane, Characterisation and blind testing of radiocarbon dating of cremated bone, J. Archaeol. Sci., 35(2008) 791–800.

[25] G. Grupe and S. Hummel, Trace element studies on experimentally cremated bone. I. Alteration of the chemical composition at high temperatures, J. Archaeol. Sci., 18(1991) 177-186.

[26] J.J. Schultz, M.W. Warren, and J.S. Krigbaum, Chapter 4. Analysis of human cremains: gross and chemical methods, in The Analysis of Burned Human Remains, San Diego: Academic Press, 2008.

[27] M. E. Subira and A. Malgosa, The effect of cremation on the study of trace elements, Int. J. Osteoarchaeol., 3(1993) 115–118.

[28] G. Gallello, J. Kuligowski, A. Pastor, A. Diez, and J. Bernabeu, Biological mineral content in Iberian skeletal cremains for control of diagenetic factors employing multivariate statistics, J. Archaeol. Sci., 40(2013) 2477–2484.

[29] L. D. Mkukuma, J. M. S. Skakle, I. R. Gibson, C. T. Imrie, R. M. Aspden, and D. W. L. Hukins, Effect of the Proportion of Organic Material in Bone on Thermal Decomposition of Bone Mineral: An Investigation of a Variety of Bones from Different Species Using Thermogravimetric Analysis coupled to Mass Spectrometry, High-Temperature X-ray Diffraction, and Fourier Transform Infrared Spectroscopy, Calcif. Tissue Int., 75(2004) 321–328.

[30] T. Leventouri, Synthetic and biological hydroxyapatites: Crystal structure questions, *Biomaterials*, 27(2006) 3339–3342.

[31] J.D. Pasteris, B. Wopenka, J.J. Freeman, K.Rogers,E. Valsami-Jones, J.A.M. van der Houwen, M.J. Silva, Lack of OH in nanocrystalline apatite as a function of degree of atomic order: implications for bone and biomaterials, Biomaterials, 25(2004) 229–238.

[32] B. Wopenka and J. D. Pasteris, A mineralogical perspective on the apatite in bone, Mater. Sci. Eng. C, 25(2005) 131–143.

[33] Apatites and their Synthetic Analogues-Synthesis, Structure, Properties and Applications, Petr Ptacek, 2016.

[34] T. J. U. Thompson, M. Gauthier, and M. Islam, The application of a new method of Fourier Transform Infrared Spectroscopy to the analysis of burned bone, J. Archaeol. Sci., 36(2009) 910–914.

[35] T. J. U. Thompson, M. Islam, K. Piduru, and A. Marcel, An investigation into the internal and external variables acting on crystallinity index using Fourier Transform Infrared Spectroscopy on unaltered and burned bone, Palaeogeogr. Palaeoclimatol. Palaeoecol., 299(2011) 168–174.

[36] M. Lebon *et al.*, New parameters for the characterization of diagenetic alterations and heat-induced changes of fossil bone mineral using Fourier transform infrared spectrometry, J. Archaeol. Sci., 37(2010) 2265–2276.

[37] J. M. Martinez Garcia, La necrópolis ibérica de Las Peñas (Zarra, Valencia), Archivo de Prehistoria Levantina., vol. XIX. Valencia, 1989.

[38] D. Ballabio, A MATLAB toolbox for Principal Component Analysis and unsupervised exploration of data structure, Chemom. Intell. *Lab. Syst.*, 149(2015), Part B, 1–9.

[39] M. J. Hidalgo, D. C. Fechner, E. J. Marchevsky, and R. G. Pellerano, Determining the geographical origin of Sechium edule fruits by multielement analysis and advanced chemometric techniques, Food Chem., 210(2016) 228–234.

[40] M. R. Almeida, C. H. V. Fidelis, L. E. S. Barata, and R. J. Poppi, Classification of Amazonian rosewood essential oil by Raman spectroscopy and PLS-DA with reliability estimation, Talanta, 117(2013) 305–311.

[41] F. B. de Santana, L. C. Gontijo, H. Mitsutake, S. J. Mazivila, L. M. de Souza, and W. Borges Neto, Non-destructive fraud detection in rosehip oil by MIR spectroscopy and chemometrics, Food Chem., 209(2016) 228–233.

[42] P.C. Williams, D. Sobering How do we do it: A brief summary of the methods we use in developing near infrared calibrations A.M.C. Daves, P.C. Williams (Eds.), Near infrared spectroscopy: The future waves, NIR Publications, Chichester, UK (1995) 185–188.

[43] R. L. Frost, B. J. Reddy, S. Bahfenne, and J. Graham, Mid-infrared and near-infrared spectroscopic study of selected magnesium carbonate minerals containing ferric iron—Implications for the geosequestration of greenhouse gases, Spectrochim. Acta. A. Mol. Biomol. Spectrosc., 72(2009) 597–604.

[44] Y. Ning, J. Li, W. Cai, and X. Shao, Simultaneous determination of heavy metal ions in water using near-infrared spectroscopy with preconcentration by nano-hydroxyapatite, Spectrochim. Acta. A. Mol. Biomol. Spectrosc., 96(2012) 289–294.

[45] V. Aranda, A. Domínguez-Vidal, F. Comino, J. Calero, and M. J. Ayora-Cañada, Agro-environmental characterization of semi-arid Mediterranean soils using NIR reflection and mid-IR-attenuated total reflection spectroscopies, Vib. Spectrosc., 74(2014) 88–97.

[46] D. Thomas, C. McGoverin, A. Chinsamy, and M. Manley, Near infrared analysis of fossil bone from the Western Cape of South Africa, J. Infrared Spectrosc., 19(2011) 151, 2011.

[47] M. Mora, M. Isabel López, M. Ángeles Carmona, C. Jiménez-Sanchidrián, and J. Rafael Ruiz, Study of the thermal decomposition of a sepiolite by mid- and near-infrared spectroscopies, Polyhedron, 29(2010) 3046–3051.

[48] K. Van Aken, L. Strekowski, L. Patiny, EcoScale, a semi-quantitative tool to select an organic preparation based on economical and ecological parameters Beilstein Journal of Organic Chemistry, 2 (2006), 3.

[49] A. Galuszka, P. Konieczka, Z.M. Migaszewski, J. Namiésnik, Analytical eco-scale for assessing the greenness of analytical procedures, Trac-Trend in Analytical Chemistry, 37 (2012), 61–72.

[50] S. Armenta, M. de la Guardia, J. Namiesnik (in press). Green Microextraction. In M. Valcarcel (Ed.), *Analytical Microextraction Techniques*. Bentham Science.

[51] M. M. Cascant, S. Rubio, G. Gallello, A. Pastor, S. Garrigues, and M. de la Guardia, Prediction of alkaline earth elements in bone remains by near infrared spectroscopy, Talanta, 162(2017) 428–434.

## Figure Captions

**Figure 1.** NIR spectra of calcined, carbonized, animal, superficial part of bones and sediment samples in the region between 9000 and 4000 cm$^{-1}$ without data pre-treatment.

**Figure 2.** Scores plot for first and second principal components obtained by PCA from NIR spectra of samples of Corral de Saus and Las Peñas Necropolis, after FD and MC pre-treatment using the region from 9000 to 4000 cm$^{-1}$.

**Figure 3.** Loadings of PC1 and PC2 after FD and MC pre-treatment of spectra using the region from 9000 to 4000 cm$^{-1}$.

**Figure 4.** Cluster dendrographic classification of bone and sediment samples based on their NIR spectra after FD and MC pre-treatment and selecting the region from 9000 to 4000 cm$^{-1}$concerning **a)** calcined, carbonized, animal, external part of bones and sediments established using average-paired distance and, **b)** calcined and carbonized bones classification using K-means nearest group as distance method.

**Figure 5.** Classification by PLS-DA of NIR spectra of bones, after FD and MC pre-treatment and selecting the region from 9000 to 4000 cm$^{-1}$.

**Figure 6.** Predicted vs reference values for PLS-NIR determination of calcium, magnesium and strontium in burned bone samples.

**Figure 7.** Green evaluation of PLS-NIR vs ICP-OES for Ca, Mg and Sr determination in bone remains.

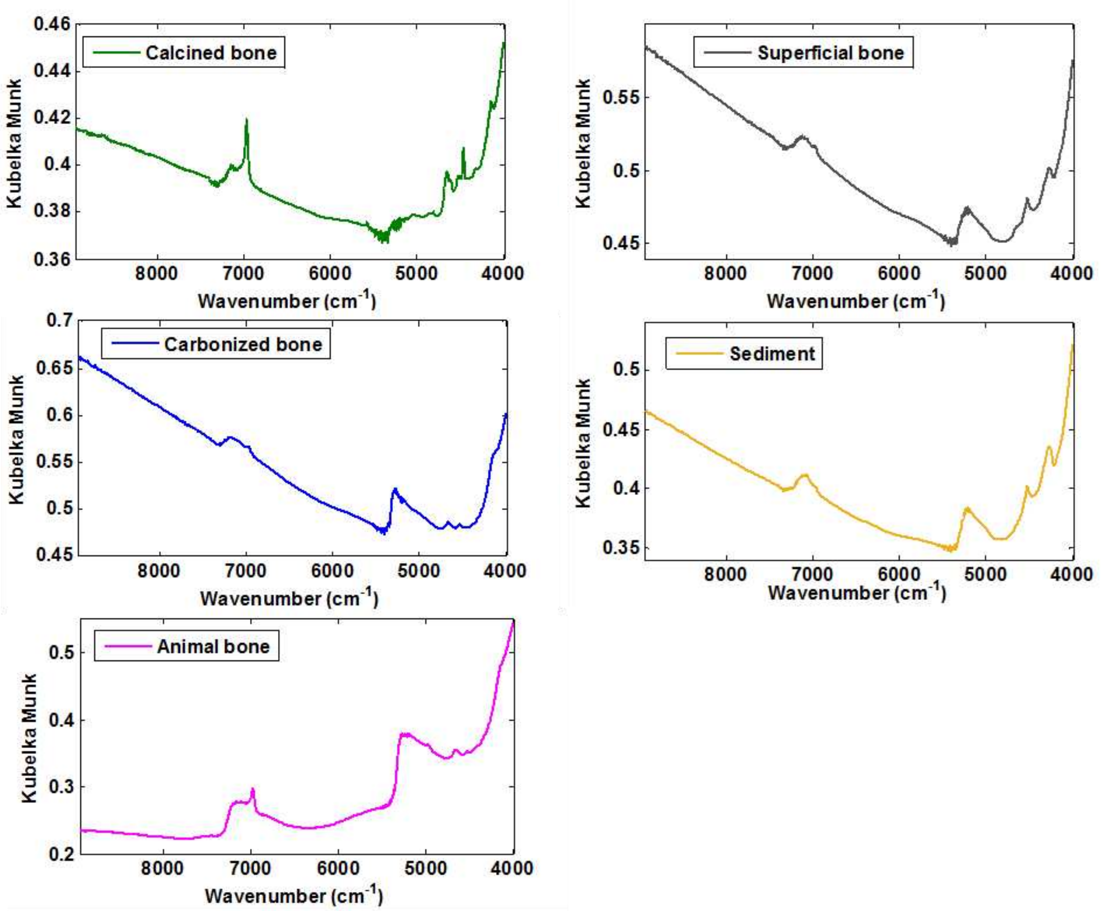
Calcined bone
Superficial bone
Carbonized bone
Sediment
Animal bone
Kubelka Munk
Wavenumber (cm$^{-1}$)
0.46
0.44
0.42
0.4
0.38
0.36
0.55
0.5
0.45
0.7
0.65
0.6
0.55
0.5
0.45
0.5
0.45
0.4
0.35
0.5
0.4
0.3
0.2
8000
7000
6000
5000
4000

FIGURE 1

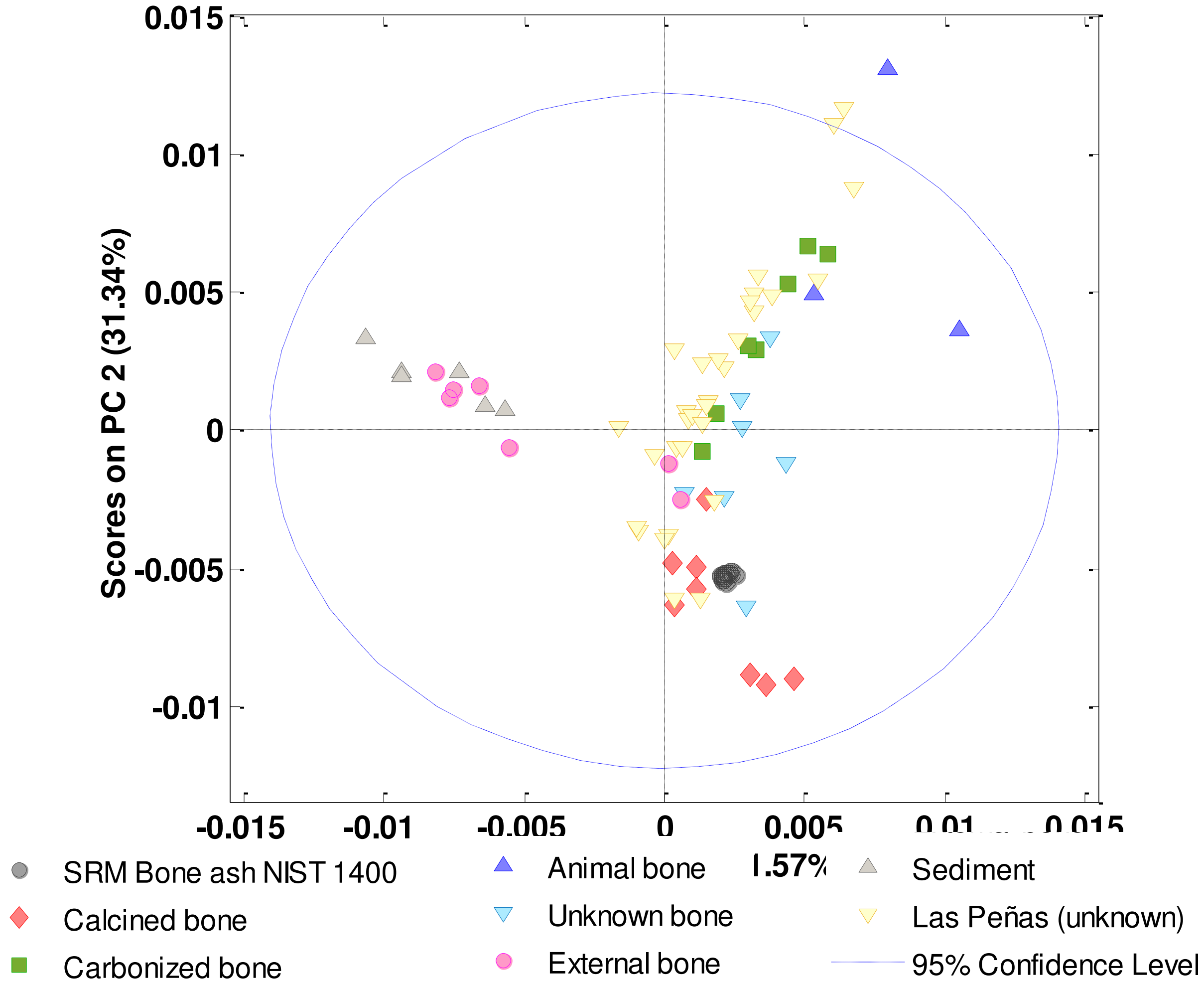

Scores on PC 2 (31.34%)
0.015
0.01
0.005
0
-0.005
-0.01
-0.015
-0.01
-0.005
0
0.005
0.01
0.015
l.57%
SRM Bone ash NIST 1400
Calcined bone
Carbonized bone
Animal bone
Unknown bone
External bone
Sediment
Las Peñas (unknown)
95% Confidence Level

FIGURE 2

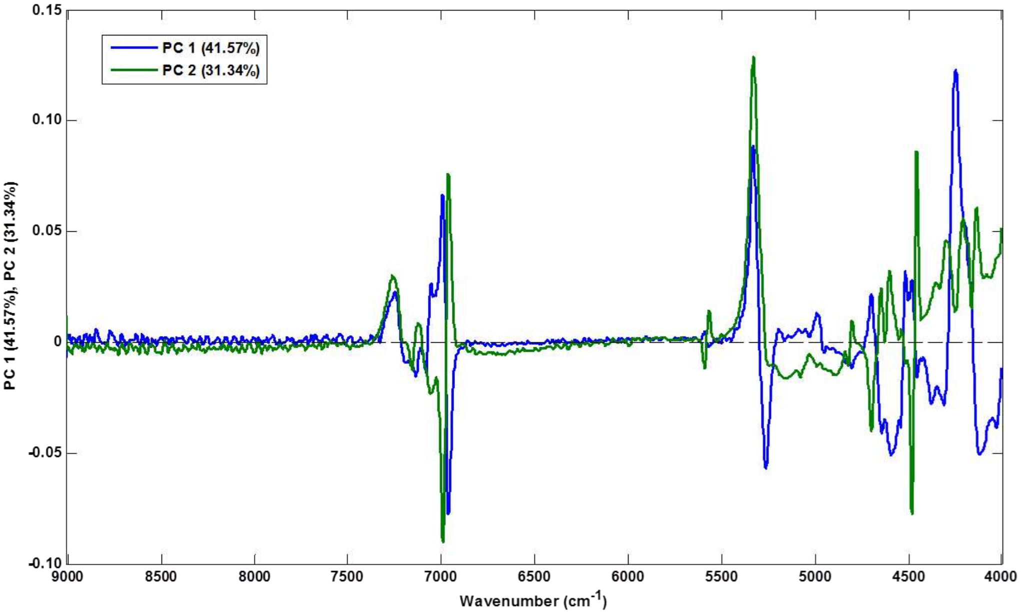

PC 1 (41.57%)
PC 2 (31.34%)
0.15
0.10
0.05
0
-0.05
-0.10
PC 1 (41.57%), PC 2 (31.34%)
9000
8500
8000
7500
7000
6500
6000
5500
5000
4500
4000
Wavenumber (cm$^{-1}$)

FIGURE 3

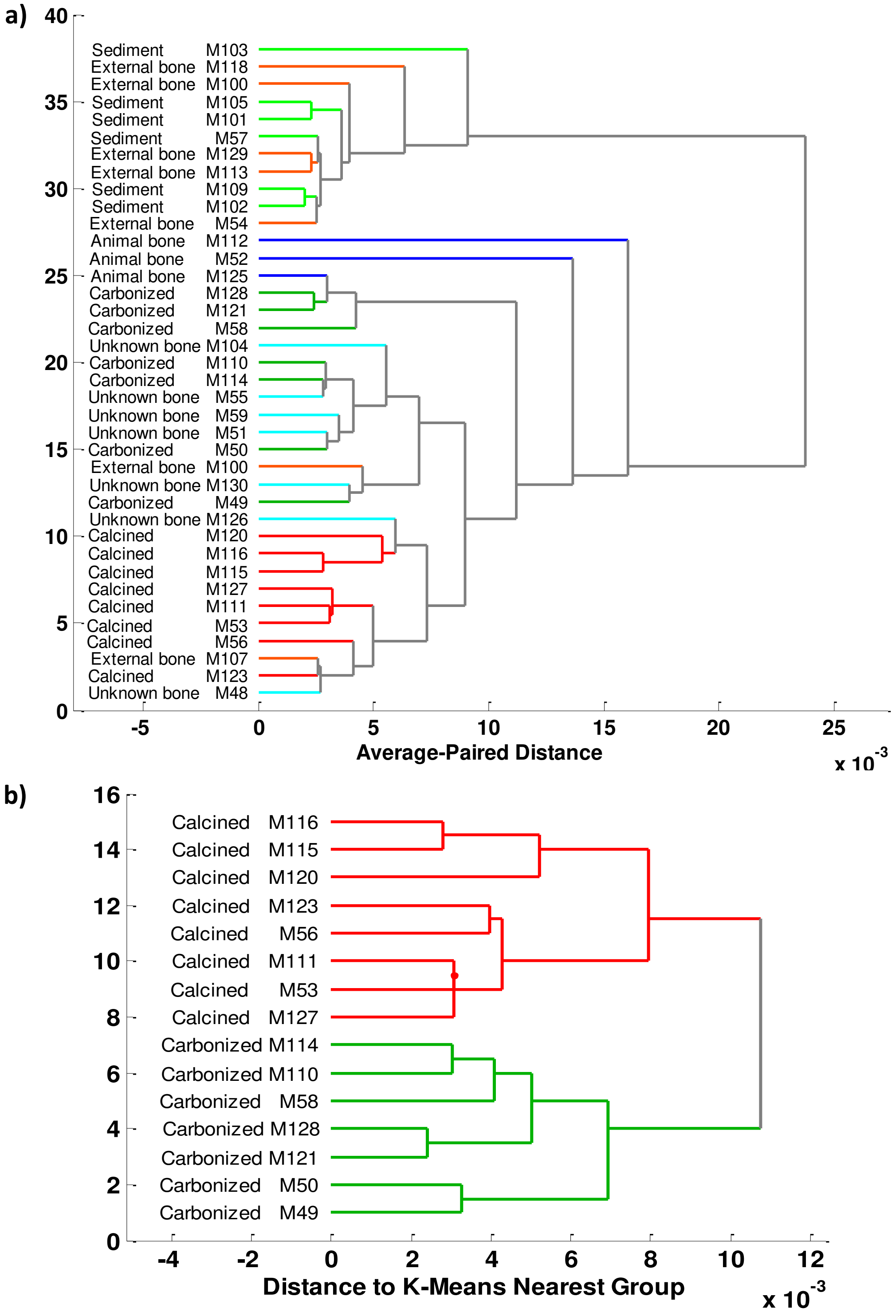

a)
Sediment M103
External bone M118
External bone M100
Sediment M105
Sediment M101
Sediment M57
External bone M129
External bone M113
Sediment M109
Sediment M102
External bone M54
Animal bone M112
Animal bone M52
Animal bone M125
Carbonized M128
Carbonized M121
Carbonized M58
Unknown bone M104
Carbonized M110
Carbonized M114
Unknown bone M55
Unknown bone M59
Unknown bone M51
Carbonized M50
External bone M100
Unknown bone M130
Carbonized M49
Unknown bone M126
Calcined M120
Calcined M116
Calcined M115
Calcined M127
Calcined M111
Calcined M53
Calcined M56
External bone M107
Calcined M123
Unknown bone M48
40
35
30
25
20
15
10
5
0
-5
0
5
10
15
20
25
Average-Paired Distance
x 10^-3
b)
Calcined M116
Calcined M115
Calcined M120
Calcined M123
Calcined M56
Calcined M111
Calcined M53
Calcined M127
Carbonized M114
Carbonized M110
Carbonized M58
Carbonized M128
Carbonized M121
Carbonized M50
Carbonized M49
16
14
12
10
8
6
4
2
0
-4
-2
0
2
4
6
8
10
12
Distance to K-Means Nearest Group
x 10^-3

FIGURE 4

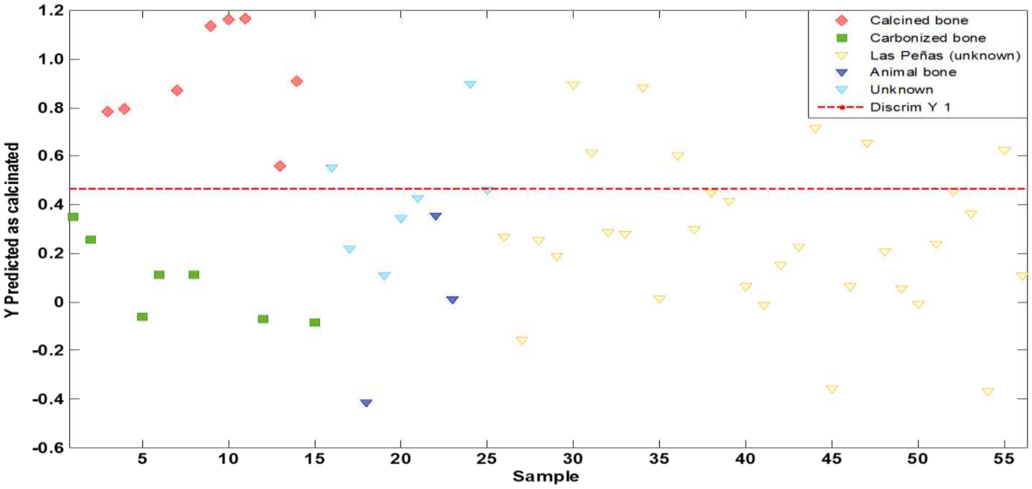
1.2
1.0
0.8
0.6
0.4
0.2
0
-0.2
-0.4
-0.6
Y Predicted as calcinated
5
10
15
20
25
30
35
40
45
50
55
Sample
Calcined bone
Carbonized bone
Las Peñas (unknown)
Animal bone
Unknown
Discrim Y 1

FIGURE 5

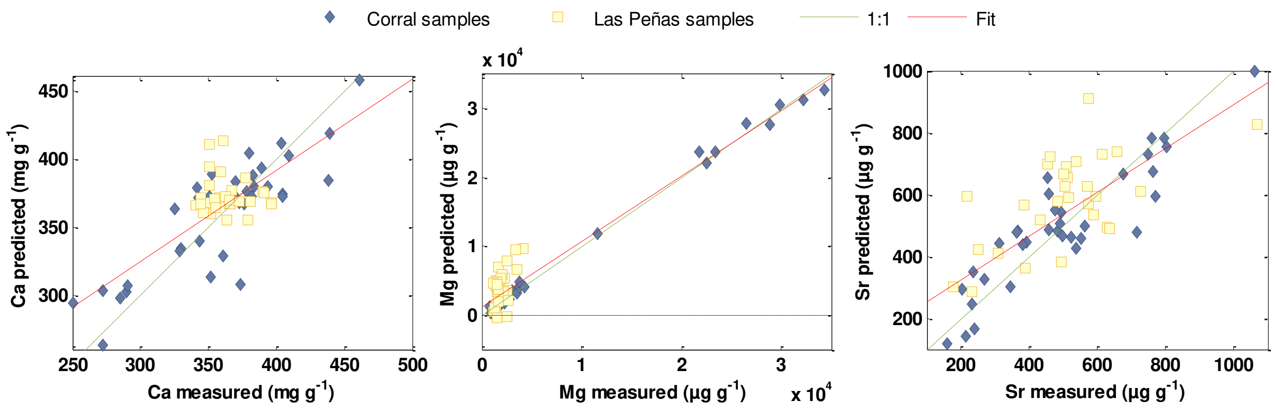
Corral samples
Las Peñas samples
1:1
Fit
Ca predicted (mg g-1)
450
400
350
300
250
300
350
400
450
500
Ca measured (mg g-1)
x 10^4
Mg predicted (µg g-1)
3
2
1
0
0
1
2
3
Mg measured (µg g-1)
x 10^4
Sr predicted (µg g-1)
1000
800
600
400
200
200
400
600
800
1000
Sr measured (µg g-1)

FIGURE 6

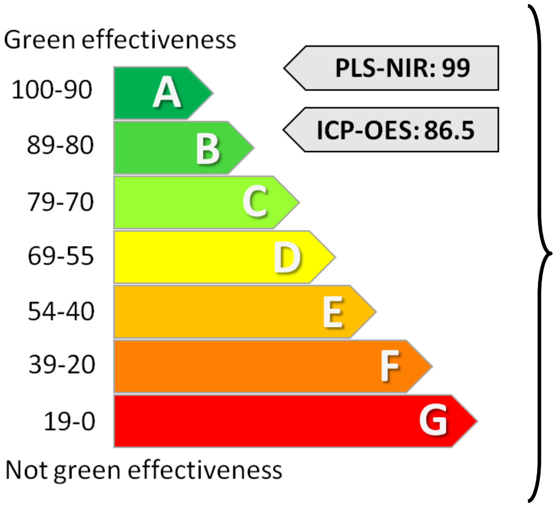

| Penalty points | PLS-NIR | ICP-OES |
|---|---|---|
| Reagents | 0 | 2 |
| Instrumental | 1 | 3 |
| Occupational hazard | 0 | 0 |
| Waste | 0 | 8.5 |
| Σ Penalty points | 1 | 13.5 |
| Green effectiveness | 99 | 86.5 |

FIGURE 7

**Table 1.** Assignation of NIR bands present in skeletal remains and sediment samples.

| Wavenumber (cm $^{-1}$) | CLN | CRB | EXT | ANM | SED | Assignments | Ref |
|---|---|---|---|---|---|---|---|
| 7197 | ● | ● | ● | ● | ● | 1st overtone of Mg-OH stretching in dioctahedral layers | [47] |
| 7070 | - | - | ● | - | ● | 1st overtone of the O–H stretch vibration in metal–O–H | [45] |
| 6977 | ● | ● | ● | ● | ● | 1st overtone stretching vibrations of OH group in hydroxyapatite | [44] |
| 5275 | - | ● | - | ● | ● | Apatite | [46] |
| 5190 | ● | ● | ● | ● | ● | Combination vibrations of H–O–H bend and O–H stretch of water | [45] |
| 4966 | - | - | - | ● | - | | |
| 4812 | ● | - | - | - | - | | |
| 4655 | ● | ● | ● | ● | - | | |
| 4619 | ● | - | - | - | - | | |
| 4530 | - | ● | ● | ● | ● | clay minerals, like smectite and illite | [44] |
| 4468 | ● | - | - | - | - | | |
| 4326 | ● | - | - | - | - | OH combination (Mg–OH, stretching + bending) | [47] |
| 4265 | - | - | ● | - | ● | contribution of calcite | [44] |
| 4150 | ● | ● | - | ● | - | | |

CLN: Calcined bone; CRB: Carbonized bone; EXT: External bone; ANM: Animal bone; SED: Sediments.

**Table 2.** Concentration ranges of major elements present in samples corresponding to calibration, and validation data set.

| Analyte | Set | Samples | Range | Mean value | SD |
|---|---|---|---|---|---|
| **Calcium (mg g$^{-1}$)** | Calibration | 35 | 250 - 461 | 360 | 49 |
| **Magnesium (µg g$^{-1}$)** | | 36 | 790 - 34257 | 8091 | 10820 |
| **Strontium (µg g$^{-1}$)** | | 35 | 161 - 1061 | 494 | 215 |
| **Calcium (mg g$^{-1}$)** | Validation | 31 | 341 - 397 | 363 | 16 |
| **Magnesium (µg g$^{-1}$)** | | 31 | 1213 - 4116 | 2014 | 711 |
| **Strontium (µg g$^{-1}$)** | | 29 | 179 - 1068 | 503 | 176 |

SD: Standard deviation

**Table 3.** Description and validation parameters of PLS-NIR models developed for the

| Element | Pre-process | LV's | RMSEC | $R^2$ Cal | RMSECV | $R^2$ CV | RMSEP | RRMSEP (%) | RPD |
|---|---|---|---|---|---|---|---|---|---|
| **Calcium ($mg\ g^{-1}$)** | FD, MC | 3 | 25.4 | 72.8 | 29.9 | 62.2 | 18.9 | 5.2 % | 0.86 |
| **Magnesium ($\mu g\ g^{-1}$)** | FD, MC | 8 | 665.7 | 99.6 | 3115.7 | 92.4 | 2941.5 | 146 % | 0.24 |
| **Strontium ($\mu g\ g^{-1}$)** | FD, MC | 3 | 92.5 | 80.9 | 112.6 | 71.8 | 162.57 | 32.3 % | 1.08 |

determination of calcium, magnesium and strontium.

LV: number of latent variables
RMSEC: Root mean square error of calibration; RMSECV: Root mean square error of cross validation; RMSEP: Root mean square error of prediction; RRMSEP: Relative root mean square error of prediction; $R^2$ Cal: coefficient of determination of calibration; $R^2$ CV: coefficient of determination of cross validation; $R^2$ Pred: coefficient of determination of prediction.

**Table 4.** Inter-day precision and accuracy parameters of the PLS-NIR methodology for the determination of calcium, magnesium and strontium in Bone ash NIST 1400.

| | **Ca** | **Mg** | **Sr** |
|---|---|---|---|
| **CV (%)** | 0.2 – 1.5 | 4.7 – 13.8 | 0.3 – 1.8 |
| **Er (%)** | (-4.3) – (-2.3) | (-26.5) – (-8.4) | 6.9 – 9.9 |

CV: coefficient of variation
Er: relative error.